

Quasi-normal mode expansion of black hole perturbation : a hyperboloidal Keldysh approach

J. Besson

joint work with P. Bizoń, V. Boyanov, J.L. Jaramillo, D. Pook-Kolb

Université de Bourgogne; Albert-Einstein-Institut (Max Planck Institut)

Table of Contents

- 1 Introduction
- 2 Compactified hyperboloidal approach
- 3 Keldysh resonant expansion
- 4 Cases of study and simulations
- 5 Pseudospectra and regularity
- 6 Conclusions

Introduction

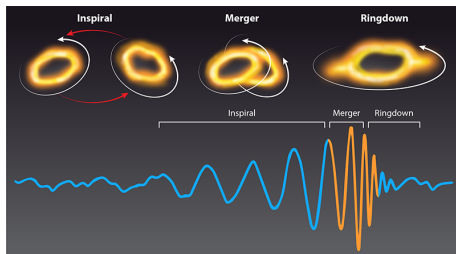


Figure: Illustration of a pair of coalescing black holes (credit : (Top) Kip Thorne; (Bottom) B. P. Abbott et al. [8]; adapted by APS/Carin Cain)

Ringdown

Sum of damped oscillators

$$\Psi_{\ell,m}(t) \sim \sum_n A_{\ell,m,n} e^{i\omega_{\ell,m,n}t}$$

Introduction : the conservative case

The conservative case

Example of system : guitar string struck

Consider the linear equation

$$\begin{cases} \partial_t u = iHu \\ u(t = 0, x) = u_0(x) \end{cases}$$

where H is self-adjoint and the eigenfunctions \hat{v}_n form an orthonormal basis of the Hilbert space. The solution can be written as a convergent sum over the harmonics

$$u(x, t) = \sum_{n=0}^{\infty} a_n \hat{v}_n(x) e^{i\omega_n t}$$

where

$$a_n = \langle \hat{v}_n, u_0 \rangle_G, \quad H\hat{v}_n = \omega_n \hat{v}_n$$

Introduction : quasinormal modes definitions and BH perturbation theory

Quasi-normal modes (QNMs)

Definition : Resonant response under linear perturbation characterized by complex frequencies. QNMs probe the background spacetime geometry
Lax-Phillips theory : QNMs as poles of the resolvent

Perturbation theory on Schwarzschild black hole

Scalar, electromagnetic and gravitational perturbations reduce to the following wave equation in the tortoise coordinates

$$\left(\frac{\partial^2}{\partial t^2} - \frac{\partial^2}{\partial r_*^2} + V_\ell(r_*) \right) \phi_{\ell m} = 0 + \text{boundary conditions}$$

where V_ℓ depends on the type of perturbation (spin $s = 0, 1$ or 2).

Introduction : quasinormal modes definitions and BH perturbation theory

Quasi-normal modes (QNMs)

Definition : Resonant response under linear perturbation characterized by complex frequencies. QNMs probe the background spacetime geometry
Lax-Phillips theory : QNMs as poles of the resolvent

Perturbation theory on Schwarzschild black hole

Scalar, electromagnetic and gravitational perturbations reduce to the following wave equation in the tortoise coordinates

$$\left(\frac{\partial^2}{\partial t^2} - \frac{\partial^2}{\partial \bar{x}^2} + \lambda^2 V_\ell(\bar{x}) \right) \phi_{\ell m} = 0 + \text{boundary conditions}$$

where V_ℓ depends on the type of perturbation (spin $s = 0, 1$ or 2).

Introducing hyperboloidal slicings

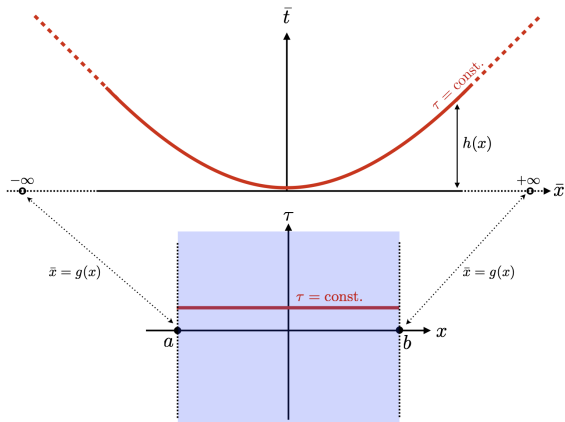


Figure: Picture of the compactified hyperboloidal coordinates (credit : [Lamis El Sheikh PhD thesis](#))

Pöschl-Teller : a toy model (part 1)

Pöschl-Teller (1/2)

$$\left(\frac{\partial^2}{\partial \bar{t}^2} - \frac{\partial^2}{\partial \bar{x}^2} + V(\bar{x}) \right) \phi = 0, \quad V(\bar{x}) = V_0 \operatorname{sech}^2(\bar{x})$$

The following change of variable^a defines a compactified hyperboloidal foliation :

$$\begin{cases} \tau = \bar{t} - \ln(\cosh \bar{x}) \\ x = \tanh^{-1}(\bar{x}) \end{cases}$$

$$\bar{t}, \bar{x} \in \mathbb{R}; x \in [-1, 1]$$

^aEl Sheikh,Jaramillo,Macedo;2004.06434, Bizoń,Chmaj,Mach;2002.01770

Introducing hyperboloidal slicings

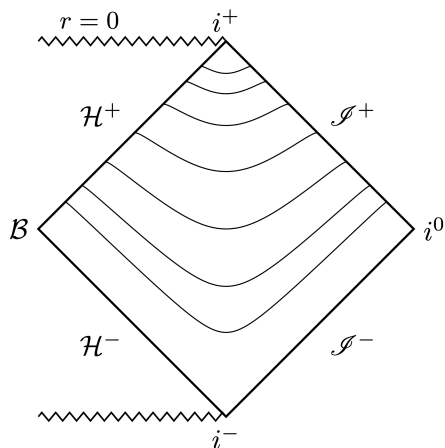


Figure: Example of hyperboloidal slicing (credit : hyperboloid.al)

Pöschl-Teller : a toy model (part 2)

Pöschl-Teller (2/2)

First order reduction : $u(x, \tau) = \begin{pmatrix} \phi \\ \psi \end{pmatrix}$ with $\psi := \partial_\tau \phi$,

$$\partial_\tau \begin{pmatrix} \phi \\ \psi \end{pmatrix} = \left(\begin{array}{c|c} 0 & 1 \\ \hline \partial_x((1-x^2)\partial_x) - V_0 & -(2x\partial_x + 1) \end{array} \right) \begin{pmatrix} \phi \\ \psi \end{pmatrix}$$

Differential equation :

$$\partial_\tau u = iLu, \quad u(x, \tau = 0) = u_0(x)$$

Spectral problem :

$$Lv_n = \omega_n v_n$$

Analytical Pöschl-Teller QNMs

$$\phi_n(x) = \text{Gegenbauer polynomials } C_n^{(i\omega_n - \frac{1}{2})}(x), \quad \omega_n = \pm \frac{\sqrt{3}}{2} + i \left(n + \frac{1}{2} \right)$$

Pöschl-Teller quasi-normal frequencies

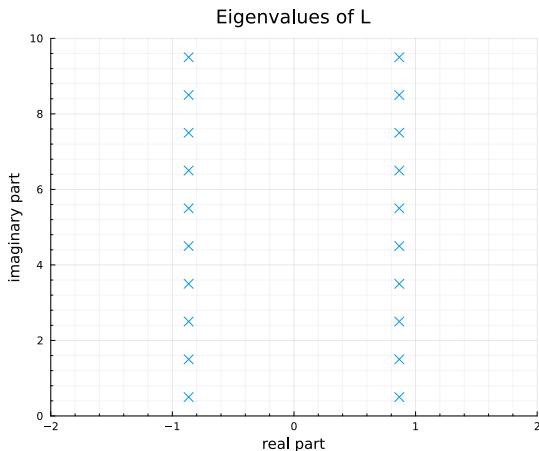


Figure: View of the Pöschl-Teller QNMs frequencies in the complex plane

Table of Contents

- 1 Introduction
- 2 Compactified hyperboloidal approach**
- 3 Keldysh resonant expansion
- 4 Cases of study and simulations
- 5 Pseudospectra and regularity
- 6 Conclusions

Compactified hyperboloidal approach

Compactified hyperboloidal slicing

$$\begin{cases} \bar{t} = \tau - h(x) \\ \bar{x} = g(x) \end{cases} \quad \begin{aligned} g: [a, b] &\rightarrow [-\infty, +\infty] \\ x &\mapsto g(x) = \bar{x} \end{aligned}$$

First order reduction

We define the field $\psi := \partial_\tau \phi$, the linear problem becomes

$$\partial_\tau \begin{pmatrix} \phi \\ \psi \end{pmatrix} = \left(\begin{array}{c|c} 0 & 1 \\ \hline L_1 & L_2 \end{array} \right) \begin{pmatrix} \phi \\ \psi \end{pmatrix}$$

Outgoing boundary conditions

- Geometric interpretation : outgoing null cones
- Analytic interpretation : singular Sturm-Liouville operator, the boundary conditions are built-in as regularity conditions

Compactified hyperboloidal approach

$$\partial_\tau \begin{pmatrix} \phi \\ \psi \end{pmatrix} = \underbrace{\begin{pmatrix} 0 & 1 \\ L_1 & L_2 \end{pmatrix}}_{iL} \begin{pmatrix} \phi \\ \psi \end{pmatrix}$$

All the space derivatives are contained within the matrix.

$$L_1 = \frac{1}{w(x)} (\partial_x(p(x)\partial_x) - q(x))$$

$$L_2 = \frac{1}{w(x)} (2\gamma(x)\partial_x + \partial_x\gamma(x))$$

where

$$w(x) = \frac{g'(x)^2 - h'(x)^2}{|g'(x)|}$$

$$p(x) = \frac{1}{|g'(x)|}$$

$$q(x) = |g'(x)|V_\ell(x)$$

$$\gamma(x) = \frac{h'(x)}{|g'(x)|}$$

Scalar product and non-selfadjointness

The energy scalar product is related to the energy-momentum tensor of a complex scalar field on a Minkowski spacetime with a potential V_ℓ .

$$\left\langle \begin{pmatrix} \phi_1 \\ \psi_1 \end{pmatrix}, \begin{pmatrix} \phi_2 \\ \psi_2 \end{pmatrix} \right\rangle_E = \frac{1}{2} \int_a^b w(x) \bar{\psi}_1 \psi_2 + p(x) \partial_x \bar{\phi}_1 \partial_x \phi_2 + q_\ell(x) \bar{\phi}_1 \phi_2 dx$$

We use this to justify that L_2 is a dissipative term and is responsible for non-self adjointness

$$L^\dagger = L + \frac{1}{i} \left(\begin{array}{c|c} 0 & 0 \\ \hline 0 & 2 \frac{\gamma(x)}{w(x)} (\delta(x-a) - \delta(x-b)) \end{array} \right)$$

Instability of the QNMs

The eigenvalues can be greatly perturbed upon a small perturbation of the potential

Table of Contents

- 1 Introduction
- 2 Compactified hyperboloidal approach
- 3 Keldysh resonant expansion**
- 4 Cases of study and simulations
- 5 Pseudospectra and regularity
- 6 Conclusions

Keldysh's expansion of the resolvent

Consider the application

$$F: \Omega \rightarrow \mathcal{L}(\mathcal{H}, \mathcal{K})$$

$$\omega \mapsto F(\omega)$$

Assume $F(\omega)$ is a Fredholm operator. The transpose application of F is

$$F(\omega)^t: \mathcal{K}^* \rightarrow \mathcal{H}^*$$

The spectral problems are rewritten

$$F(\omega_n)v_n = 0, \quad F(\omega_n)^t\alpha_n = 0, \quad v_n \in \mathcal{H}, \alpha_n \in \mathcal{K}^*$$

Keldysh's theorem gives an expansion of the resolvent applicationⁱ.

$$F^{-1}(\omega) = \sum_{\omega_n \in \Omega_0} \frac{\langle \tilde{\alpha}_n, \cdot \rangle}{\omega - \omega_n} v_n + H(\omega) \quad \text{with} \quad \left\langle \tilde{\alpha}_n, \frac{dF}{d\omega}(\omega_n)(v_n) \right\rangle = 1.$$

ⁱBeyn, Latushkin, Rottmann-Matthes; 1210.3952

Keldysh's resonant expansion for non-generalized eigenvalue problems

We use the recipe with $F(\omega) = L - \omega I$, the spectral problems are :

$$(L - \omega_n I)v_n = 0, \quad (L^t - \omega_n I)\alpha_n = 0, \quad v_n \in \mathcal{H}, \alpha_n \in \mathcal{H}^*$$

The resolvent of L is constructed in a bounded domain Ω can be written

$$R_L(\omega) = (L - \omega I)^{-1} = \sum_{\omega_n \in \Omega_0} \frac{\langle \tilde{\alpha}_n, \cdot \rangle}{\omega - \omega_n} v_n + H(\omega)$$

On the other hand, the Laplace transform of the differential equation yields

$$(L - \omega)u(x, \omega) = iu_0(x)$$

The asymptotic resonant expansion is then found by multiplication by the resolvent and inverse Laplace transform

$$u(\tau, x) \sim \sum_n \langle \alpha_n, u_0 \rangle v_n(x) e^{i\omega_n \tau}, \quad \text{with } \langle \alpha_n, v_n \rangle = 1$$

Asymptotic resonant expansion

Bound of the error of the Keldysh expansion

Given a bounded domain Ω in \mathbb{C} and $R = \max_{\omega \in \Omega} \text{Im}\{\omega\}$, we have

$$u(\tau, x) = \sum_{\text{Im}\{\omega_n\} \leq R} \langle \alpha_n, u_0 \rangle v_n(x) e^{i\omega_n \tau} + E_R(\tau; u_0)(x)$$

with

$$\|E_R(\tau; u_0)\|_E \leq \|u_0\|_E C_R(L) e^{-R\tau}$$

Notation

$$\mathcal{A}_n(x) = \langle \alpha_n, u_0 \rangle v_n(x), \quad \text{with } \langle \alpha_n, v_n \rangle = 1$$

$$\mathcal{A}_n^\infty = \mathcal{A}_n(x)|_{x=\text{null infinity}}$$

Table of Contents

- 1 Introduction
- 2 Compactified hyperboloidal approach
- 3 Keldysh resonant expansion
- 4 Cases of study and simulations**
- 5 Pseudospectra and regularity
- 6 Conclusions

Cases of study

Pöschl-Teller (toy model)

$$x \in [-1, 1]$$

$$\begin{cases} h(x) = \log(1 - x^2) \\ g(x) = \operatorname{arctanh}(x) \end{cases}$$

Schwarzschild

$$\sigma \in [0, 1], \lambda = 4M.$$

$$\begin{cases} h(\sigma) = \frac{1}{2} (\log \sigma + \log(1 - \sigma) - \frac{1}{\sigma}) \\ g(\sigma) = \frac{1}{2} (\frac{1}{\sigma} + \log(1 - \sigma) - \ln \sigma) \end{cases}$$

$$L_1 = \frac{1}{2(1 + \sigma)} [\partial_\sigma (2\sigma^2(1 - \sigma)\partial_\sigma) - 2\ell(\ell + 1) - (1 - s^2)\sigma]$$

$$L_2 = \frac{1}{2(1 + \sigma)} [2(1 - 2\sigma^2)\partial_\sigma - 4\sigma]$$

Cases of study

Cases	$f(r)$	potential for $s = 0, 1$ or 2 odd (axial perturbations)	potential for $s = 2$ even (polar perturbations)
Pöschl-Teller (toy model)		$V_0 \operatorname{sech}^2\left(\frac{r}{b}\right)$	
Schwarzschild	$1 - \frac{2M}{r}$	$f(r) \left(\frac{\ell(\ell+1)}{r^2} + (1-s^2) \frac{2M}{r^3} \right)$	$f(r) \frac{2}{r^3} \frac{9M^3 + 3c^2 M r^2 + c^2(1+c)r^3 + 9M^2 c r}{(3M+cr)^2}$
Schwarzschild-(Anti) de Sitter	$1 - \frac{2M}{r} - \frac{\Delta r^2}{3}$	$f(r) \left[\frac{\ell(\ell+1)}{r^2} + (1-s^2) \left(\frac{2M}{r^3} - \frac{2-s}{3} \Lambda \right) \right]$	$\frac{2f(r)}{r^3} \frac{9M^3 + 3c^2 M r^2 + c^2(1+c)r^3 + 3M^2(3cr - \Lambda r^3)}{(3M+cr)^2}$

Table 1 . Expressions for the potential in the three cases we cover. In these expressions, the cosmological constant may be positive or negative. We denote $c = \frac{(\ell-1)(\ell+2)}{2}$.

Schwarzschild-de Sitter

p vanish linearly at the event horizon and at the cosmological horizon, its expression depends on the surface gravity^a

^aSarkar, Rahman, Chakraborty; 2304.06829

Schwarzschild-Anti de Sitter

Reflexive (Dirichlet) boundary conditions imposed at the AdS boundary : acts like a box that confines the field. There are only dissipations at the event horizon^a

^aBoyanov, Cardoso, Destounis, Jaramillo; 2312.11998

Numerical methods

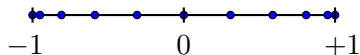


Figure: Chebyshev-Lobatto grid,
 $x_j = \cos\left(\frac{\pi j}{N}\right)$

The discretized counterpart of ϕ is a vector with $N + 1$ entries :

$$\begin{bmatrix} \phi_1 \\ \phi_2 \\ \vdots \\ \phi_N \\ \phi_{N+1} \end{bmatrix}, \quad \phi(x_j) = \phi_j$$

Numerical instability : we work with arbitrary precision numerics,

$$L : (2N + 2) \times (2N + 2) \text{ entries (matrix)}$$

$$u : (2N + 2) \text{ entries (vector)}$$

Time evolutions

Sector	Parameter
Chebyshev-Lobatto grid size	N
arbitrary decimal precision	precision
	dt increment
ODE/DAE solver (numerical time evolution)	tolerance
	algorithm

Note. — The decimal precision controls the arithmetic precision of real or complex floating numbers. The solver's dt is fixed to 10^{-7} . The precision of the ODE solver is controlled by a parameter named "tolerance". Furthermore, the solver requires an algorithm that corresponds to the discretization scheme of the time derivative. we chose to exploit Julia's automatic stiffness detection feature and we figured out the best choice in terms of accuracy and execution time is probably `AutoVern9(Rodas5P())`.

Figure: Parameters for the simulations

Time evolutions

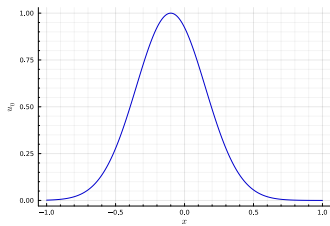
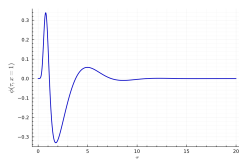
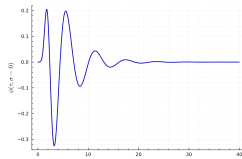


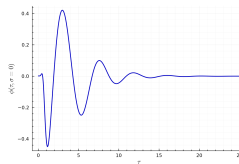
Figure: Initial data



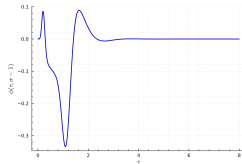
(a) Pöschl-Teller



(b) Schwarzschild-dS



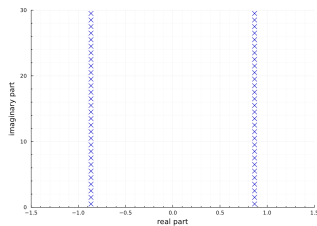
(c) Schwarzschild



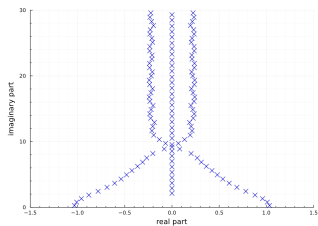
(d) Schwarzschild-AdS

Figure: Waveforms at future null infinity (event horizon for the AdS case)

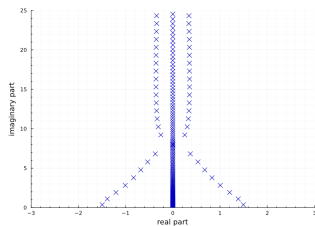
Spectra



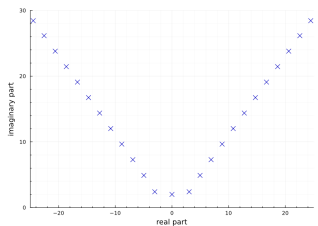
(a) Pöschl-Teller



(b) Schwarzschild-dS



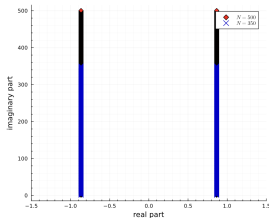
(c) Schwarzschild



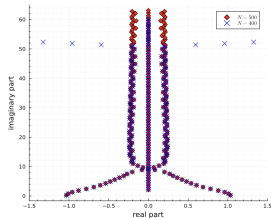
(d) Schwarzschild-AdS

Figure: Spectra of the cases of study (event horizon for the AdS case)

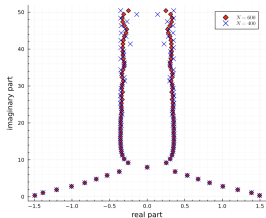
Spectra



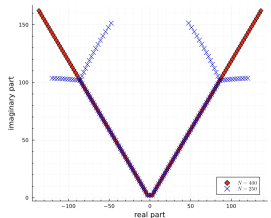
(a) Pöschl-Teller



(b) Schwarzschild-dS



(c) Schwarzschild



(d) Schwarzschild-AdS

Figure: Spectra of the cases of study for different gridsizes N

Comparing the time and the spectral domain analysis

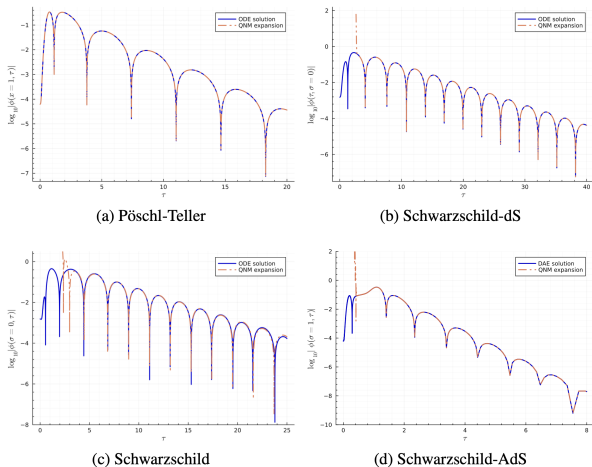


Figure: We compare the ODE solution and the Keldysh QNM expansion at future null infinity (event horizon for the AdS case)

Comparing the time and the spectral domain analysis

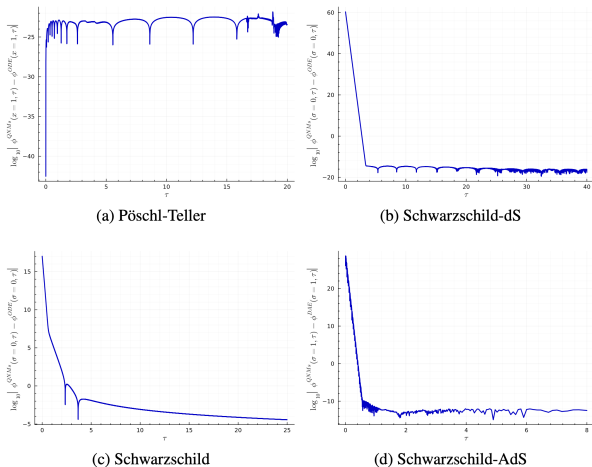
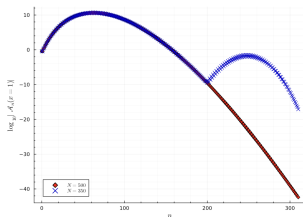
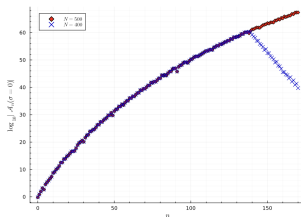


Figure: Difference between the ODE solution and the Keldysh QNM expansion at future null infinity

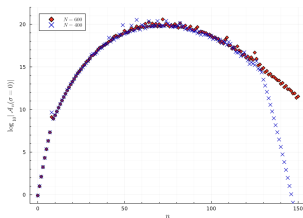
Coefficients of the timeseries at future null infinity



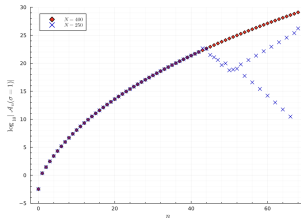
(a) Pöschl-Teller



(b) Schwarzschild-dS



(c) Schwarzschild



(d) Schwarzschild-AdS

Figure: Log plot of the modulus of the coefficients \mathcal{A}_n^∞

Schwarzschild case : separating tails and QNMs

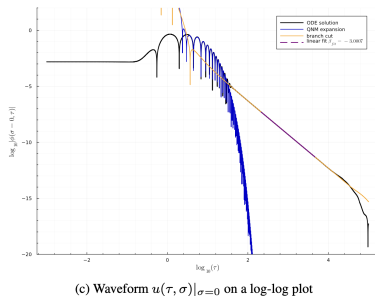
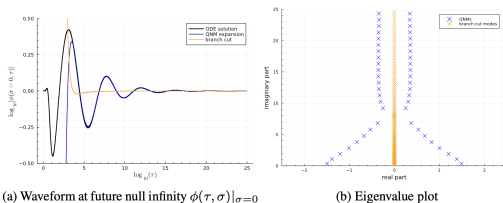


Figure: Separating tails and QNMs

Polynomial tails and branch cut modes

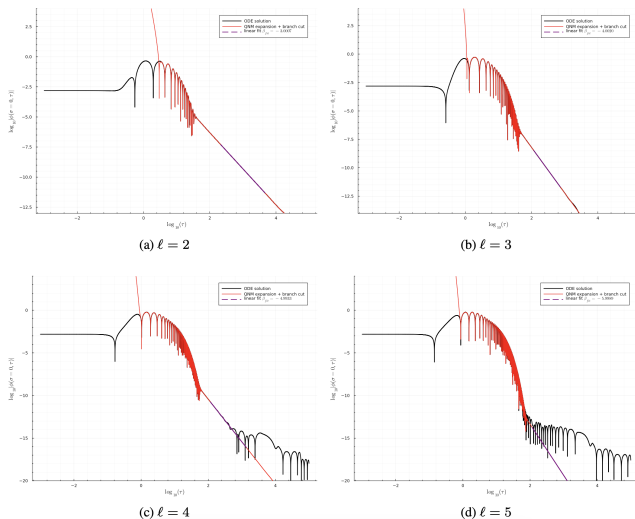


Figure: Polynomial tails in the Schwarzschild case

Role of overtones : Pöschl-Teller

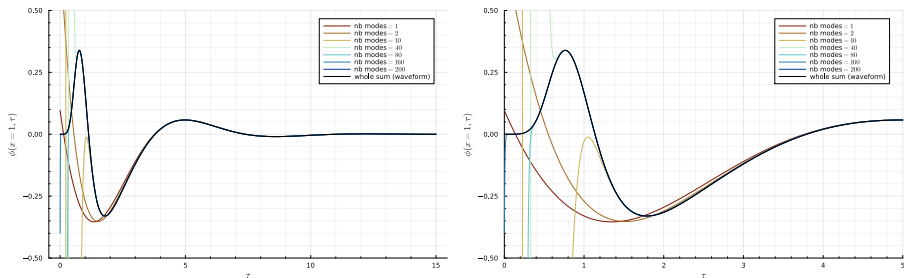


Figure: We show we recover the early times of the waveform by adding enough overtones. The panel on the right is a zoom.

Completeness ? We can describe the waveform using 310 modes with a maximum error $\approx 10^{-40}$, this begs the question whether the sum is convergent or not. What meaning do we give to the word "convergent" here ?

Role of overtones : Pöschl-Teller

$$u(\tau, x) = \sum_{\text{Im } \omega_n \leq R} \mathcal{A}_n(x) e^{i\omega_n \tau} + E_R(\tau; u_0)(x), \quad \|E_R(\tau; u_0)\|_E \leq \|u_0\|_E C_R(L) e^{-R\tau}$$

We plot $\|E_R(\tau; u_0)\|_E$ as a function of R , does

$$\forall \varepsilon > 0, \exists M \in \mathbb{N}, \forall n > M, \|E_R(\tau; u_0)\|_E < \varepsilon?$$

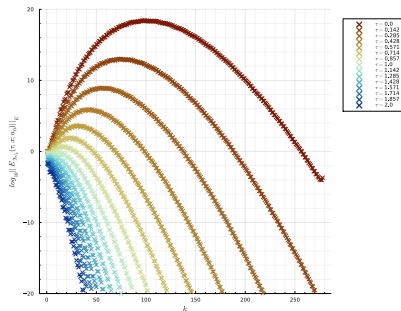
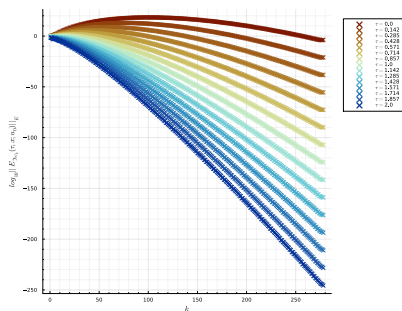


Figure: Norm of the error as we add more terms to the QNM expansion. A color corresponds to a time τ .

Table of Contents

- 1 Introduction
- 2 Compactified hyperboloidal approach
- 3 Keldysh resonant expansion
- 4 Cases of study and simulations
- 5 Pseudospectra and regularity**
- 6 Conclusions

Pseudospectrum

Given a perturbation δL of L of norm ε , what is the set of complex numbers λ which are actual eigenvalues of some perturbed operator $L + \delta L$?

Perturbative approach

$$\sigma^\varepsilon(L) = \{\lambda \in \mathbb{C}, \exists \delta L \in M_n(\mathbb{C}), \|\delta L\| < \varepsilon : \lambda \in \sigma(L + \delta L)\}$$

Resolvent norm approach

$$\sigma^\varepsilon(L) = \{\lambda \in \mathbb{C} : \|R_L(\lambda)\| = \|(\lambda I - L)^{-1}\| > 1/\varepsilon\}$$

Pseudospectrum

The colors correspond to $\log_{10} \varepsilon$.

The contour lines form circles centered on the eigenvalues and horizontal lines far away from the eigenvalues.

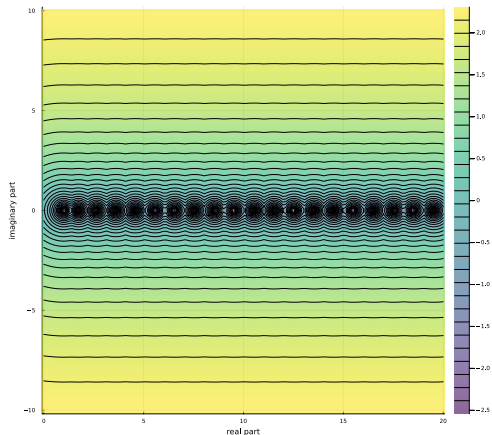


Figure: Pseudospectrum in the self adjoint case.

Pseudospectrum

The contour lines are open and the eigenvalue can migrate very far from the eigenvalues of the non perturbed operator.

Issue : The (numerical) pseudospectrum doesn't converge with N

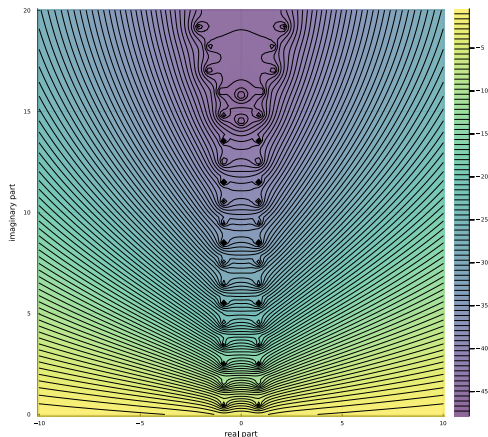


Figure: Pöschl-Teller pseudospectrum.

H^p -pseudospectrum

H^p -QNMs

H^p -QNMs are eigenfunctions of the H^p -regular operator

$$L_p: H^p \times H^{p-1} \rightarrow H^p \times H^{p-1}$$

$$(\phi, \psi) \mapsto L(\phi, \psi)$$

they constitute a finite set below $\text{Im}(\lambda) < a + \kappa \left(p - \frac{1}{2}\right)$ with κ the surface gravity and some constant a . QNMs contained in the first p bands of width κ are required to have H^p regularity. We introduce a norm that make the Pöschl-Teller pseudospectrum converge in bands and increases the regularity of the QNMs in these bands.^a

^aWarnick;1306.5760, Boyanov,Cardoso,Destounis,Jaramillo;2312.11998

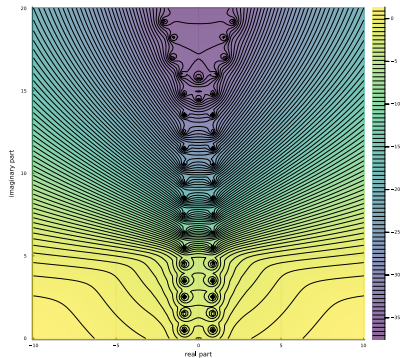


Figure: H^5 -pseudospectrum.

H^p -pseudospectrum

H^p -QNMs

H^p -QNMs are eigenfunctions of the H^p -regular operator

$$L_p: H^p \times H^{p-1} \rightarrow H^p \times H^{p-1}$$

$$(\phi, \psi) \mapsto L(\phi, \psi)$$

they constitute a finite set below $\text{Im}(\lambda) < a + \kappa(p - \frac{1}{2})$ with κ the surface gravity and some constant a . QNMs contained in the first p bands of width κ are required to have H^p regularity. We introduce a norm that make the Pöschl-Teller pseudospectrum converge in bands and increases the regularity of the QNMs in these bands.^a

^aWarnick;1306.5760, Boyanov,Cardoso,Destounis,Jaramillo;2312.11998

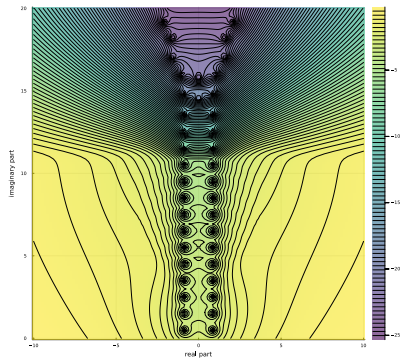


Figure: H^{11} -pseudospectrum.

Convergence of the H^p -pseudospectrum

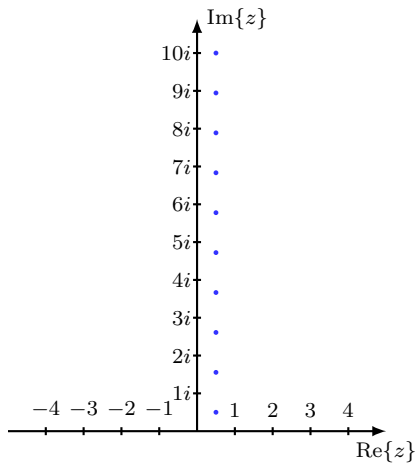


Figure: We pick some points in the complex plane

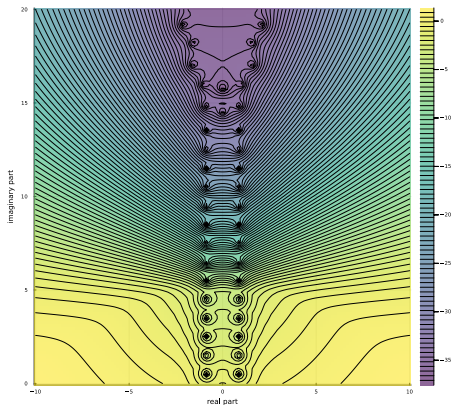


Figure: H^5 -pseudospectrum

Convergence of the H^1 -pseudospectrum

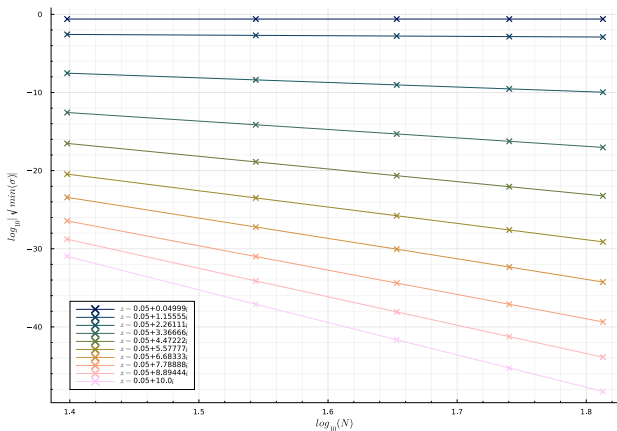


Figure: Norm of the resolvent for the H^1 norm and different z in the complex plane.

Convergence of the H^2 -pseudospectrum

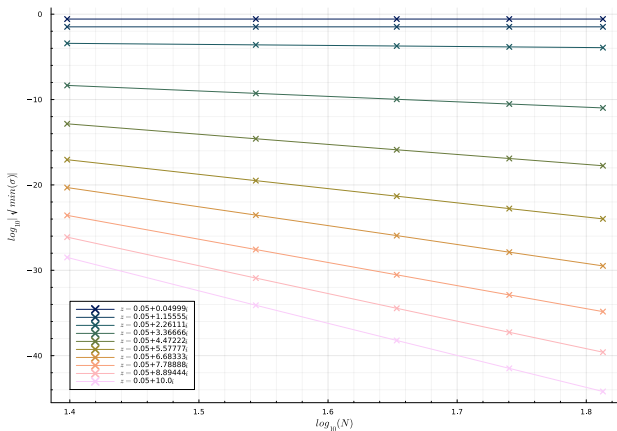


Figure: Norm of the resolvent for the H^2 norm and different z in the complex plane.

Convergence of the H^3 -pseudospectrum

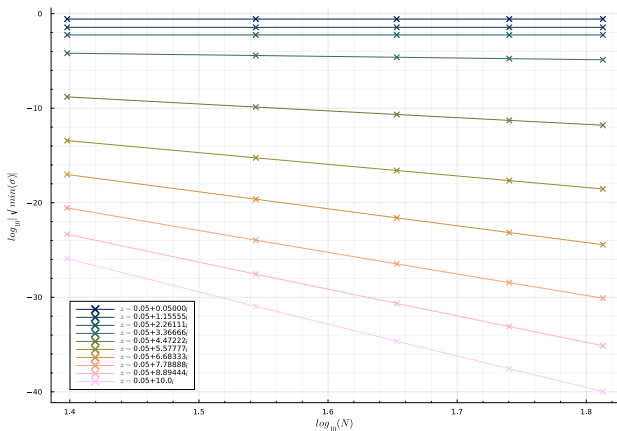


Figure: Norm of the resolvent for the H^3 norm and different z in the complex plane.

Convergence of the H^4 -pseudospectrum

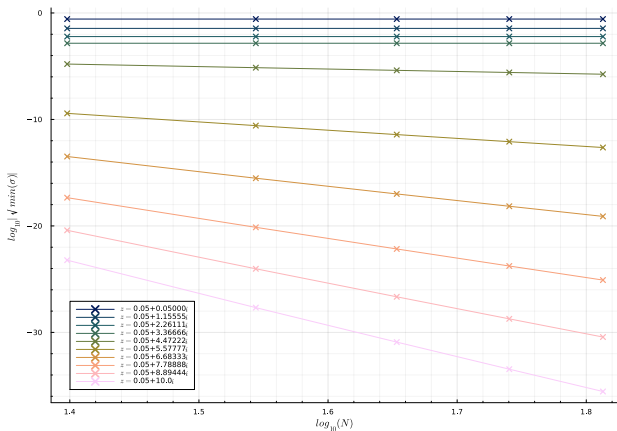


Figure: Norm of the resolvent for the H^4 norm and different z in the complex plane.

Convergence of the H^5 -pseudospectrum

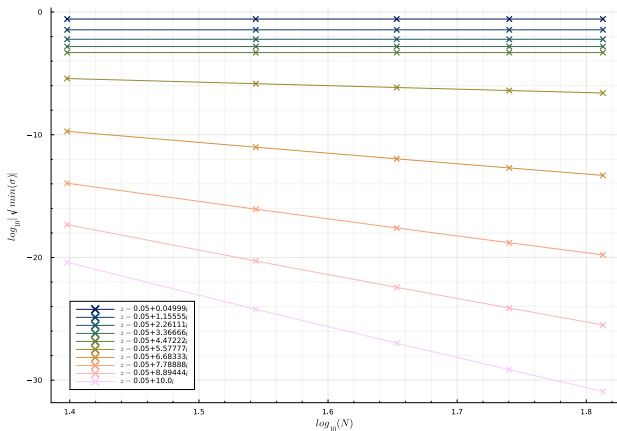


Figure: Norm of the resolvent for the H^5 norm and different z in the complex plane.

Convergence of the H^6 -pseudospectrum

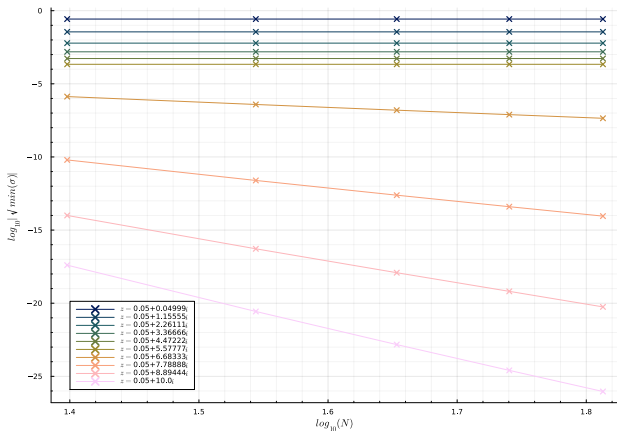


Figure: Norm of the resolvent for the H^6 norm and different z in the complex plane.

Convergence of the H^7 -pseudospectrum

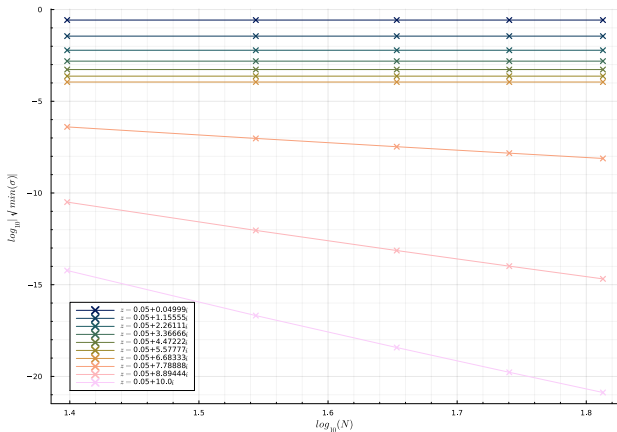


Figure: Norm of the resolvent for the H^7 norm and different z in the complex plane.

Convergence of the H^8 -pseudospectrum

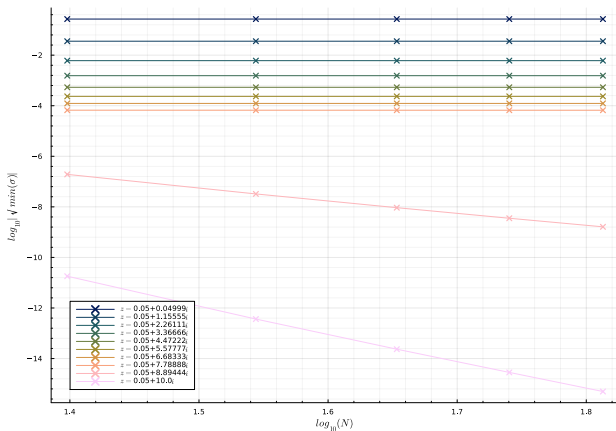


Figure: Norm of the resolvent for the H^8 norm and different z in the complex plane.

Convergence of the H^9 -pseudospectrum

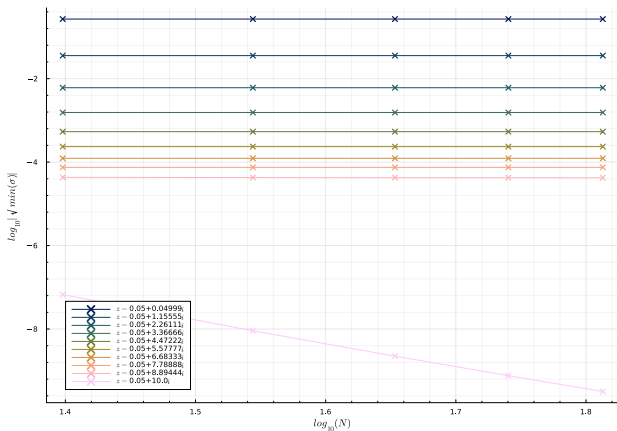


Figure: Norm of the resolvent for the H^9 norm and different z in the complex plane.

Convergence of the H^{10} -pseudospectrum

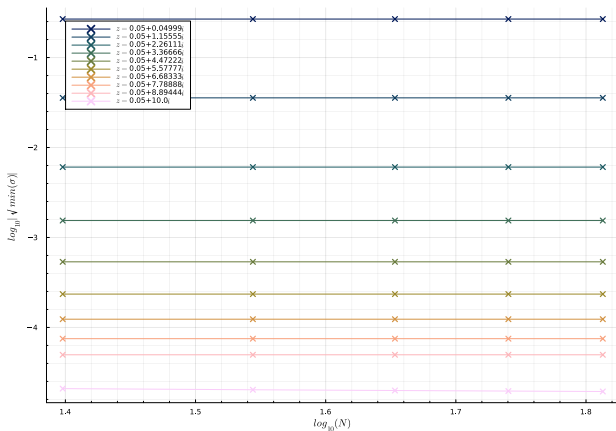


Figure: Norm of the resolvent for the H^{10} norm and different z in the complex plane.

Qualitative control of QNMs? Coefficients a_n

Notations : $\mathcal{A}_n(x) = a_n \hat{v}_n(x)$ where the v_n are the normalized eigenfunctions of L .

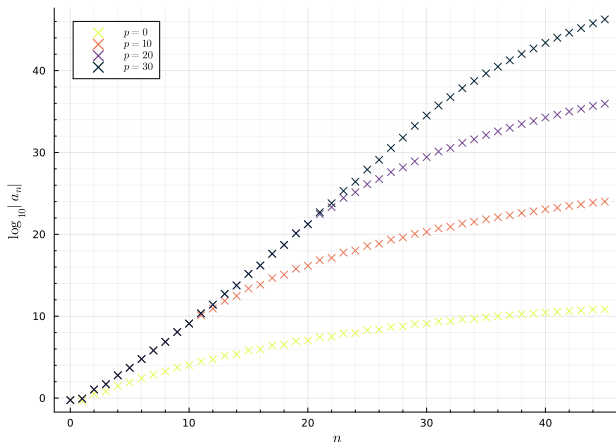


Figure: Coefficients a_n for various H^p norms.

Table of Contents

- 1 Introduction
- 2 Compactified hyperboloidal approach
- 3 Keldysh resonant expansion
- 4 Cases of study and simulations
- 5 Pseudospectra and regularity
- 6 Conclusions**

Conclusions

- Agnostic nature of the Keldysh QNM expansion : the expansion is independant of a scalar productⁱⁱ
- Unique expansion at null infinity
- Role of overtones at early times of the waveforms
- H^p –pseudospectra converge according to Warnick's criterion
- Polynomial tails are recovered and follow the Price law

ⁱⁱ [Gasperín, Jaramillo; 2107.12865](#)